

Real Time Analysis of the Contact Electrical Environment During Switching.

B.J.Frost CEng MIEE

Managing Director, Applied Relay Testing Ltd, England

Abstract - Applied Relay Testing Ltd is a specialist Company working in the field of relay device measurement, particularly for high-speed production testing. In recent times, high-end test equipment has evolved from making simple single analogue measurements on parameters towards a 'mixed-signal' approach that captures time-variant data resulting in more information and a number of spin-off benefits to the end-user of the equipment. In the context of the electrical environment of a relay contact during switching, this paper examines the techniques involved in capturing and processing such data, and the benefits that result.

I. DIGITAL SIGNAL PROCESSING APPLIED TO CONTACT MEASUREMENT – A BACKGROUND

Applied Relay Testing has been utilising the technique of Digital Signal Processing 'behind the scenes' within its relay test equipment for some years now [2]. The principle involved in such processing is now well understood and is based on taking a number of measurement samples of a parameter at short intervals and then processing the resulting data series in some way, often to derive a filtered average value. This process confers a number of benefits on most measurement situations such as allowing the trade-off of measurement quality against speed of testing and of reducing the actual measurement hardware required. A typical digital signal processing implementation is that shown in the architecture of our RT290 test system in Fig 2.

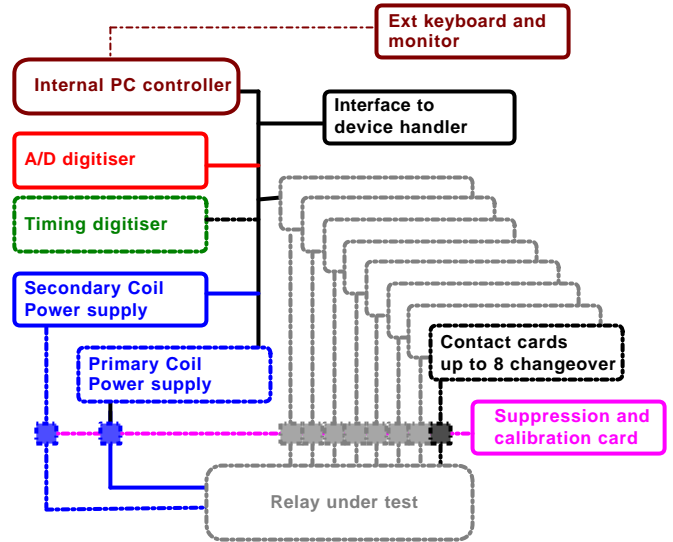


Figure 2. RT290 Internal Architecture

Based on the success of such sampled data techniques within our equipment we have investigated extending the technique to monitor the contact electrical environment during the entire contact switching process and to assess the benefits that might result.

II. SAMPLING THE CONTACT ENVIRONMENT DURING DEVICE SWITCHING

The illustrative diagram of Fig 3 is probably familiar to most relay engineers.



Figure 1. RT290 Parametric Test System.

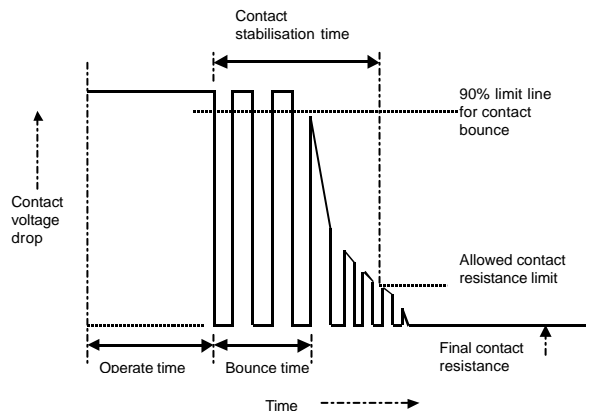


Figure 3. Generic contact switching illustration as shown in many relay specifications.

This diagram is published in many of the relay test specifications such as CECC 16000, MIL-R-39016, MIL-R-28776C etc [1] and shows the relationship between contact timing and contact resistance as might be seen in reality by displaying the actual contact voltage drop waveform on an oscilloscope. Not only is this waveform useful for clearly showing the requirements of the standards documentation but of course it is reproduced from original actual waveforms seen when such measurements were actually made by using an oscilloscope. (Indeed there are some production situations today where this practice continues and is of benefit). In the 1970's and 1980's as automatic test equipment took over from hand testing, their test method implementations typically used analogue to digital converters to perform single 'multi-meter' type measurements that neatly divide each required parameter group into individual device tests such as a 'Timing test' and a 'Contact resistance test'. Today, with the computational power available and the fall in cost of high-speed sampling hardware, it is possible to move back towards test methods that are more 'visual' in nature and therefore correspond more closely to the waveform of Fig 3 and to derive parametric result values directly from it.

So, what is point of doing this? Surely existing test equipment does a fine job by measuring each parameter separately? To a large degree this is true of course, but it turns out that there are a surprising number of benefits in taking a fresh look at contact switching measurements made in this way. Amongst these benefits are:

- a) Faster device testing.
- b) Traceability between production and laboratory.
- c) Simplicity of test method.
- d) Allows visual pass / fail limits programming.
- e) New options for contact qualification.
- f) Scales smoothly to life-testing requirements.

Some of these actually blur into one another but we will try to separate them and to examine them in more detail.

A. *Faster testing.*

The data that can be extracted from a single waveform as in Fig 3 when captured simultaneously from each contact of a device is actually equivalent to at least three main discrete device tests as implemented on traditional test equipment:

1. Timing test.
2. Contact resistance test.
3. Contact stabilisation time.

In the traditional measurement situation each of these tests would require one or more device operations. With the captured data of Fig 3 available after only one single device operation, we can apply software algorithms to extract the required result parameters, for example all of the contact timing results and all of the contact resistance values.

The contact stabilisation time test may be a luxury in that it is only sometimes needed 100% in production, but even if only the basic timing and contact resistance tests are required, their combined time is 150-200 ms compared with our new capture and processing time from the single waveform of only some 50ms – giving us at least a 3x test speed gain.

B. *Traceability between production and the laboratory.*

Employing this waveform as a standard measurement method relies on being able to link its captured graphical data to real-world relay device parameters. If this can be achieved, the entire test data flow is ideal to support the close measurement ties between the needs of production and the more analytical measurements made in the laboratory, since the basic device measurement is essentially that which would always be most desired in a laboratory situation – a visual graph. The fact that the production measurements have been subsequently extracted from this graph gives us the security of knowing that what we 'see' is directly linked to the pass / fail values obtained, allowing us to perform investigations into production device failures without regard to considerations of any differing measurement environments or test methods.

C. *Simplicity of test method.*

Displaying contact parameters using a graph gives probably the ultimate in WYSIWYG ("What You See Is What You Get") testing. Because the actual interaction with the device is so simple and the overall waveform result so easy to observe, any 'test methods' that subsequently link this captured data to the final result parameters are simply intuitive algorithms that work together with graphical limit 'lines' and which are thus close to those described by the standards documentation, so there is a much stronger tie between how the testing is being done and the traditional definitions of how it should be done.

D. *Allows visual pass / fail limits programming.*

Allied with 'C' – the 'simplicity' of the testing – comes another benefit – the ability to define test limits in a visual way. Suitable software easily permits a limit box to be included on the captured data showing both the limits that apply and allowing them to be moved where desired.

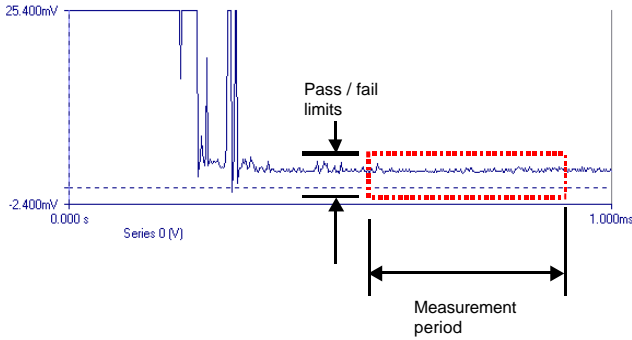


Figure 4. Contact resistance measurement parameters illustrated and adjusted graphically

For example Fig 4 shows how easy it is to indicate on the captured plot the actual final contact resistance limits and measurement duration. Note too, that it is quite easy to take contact resistance measurement a stage further and link the start of the measurement duration to the observed operate time and to ensure therefore that devices are always measured after the contact has stabilised for a sufficient time instead of risking inadvertent measurement during contact stabilisation.

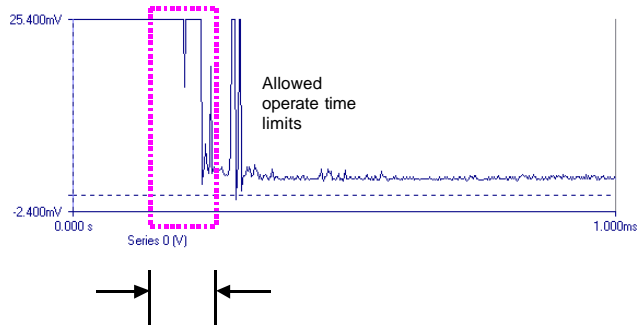


Figure 5. Timing measurement parameters illustrated and adjusted graphically

In the same way, an allowed timing limit box can easily be superimposed on the observed data as shown in Fig 5. The same techniques apply to bounce time and contact stabilisation time.

E. New options for contact qualification.

Because there is so much more information contained in this captured waveform, it is possible to define new ‘test types’ that confirm or quantify contact characteristics that were only previously possible when an operator visually confirmed pass / fail criteria by inspecting the display on an oscilloscope.

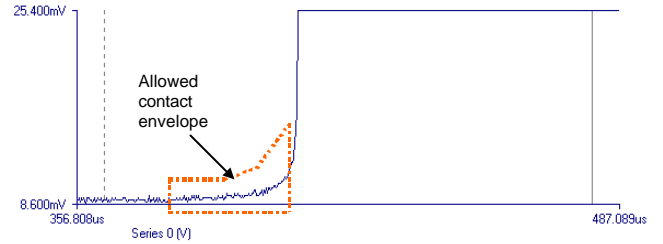


Figure 6. An example of a ‘permitted’ contact resistance envelope.

For example, consider the waveform capture of fig 6 which shows a reed switch contact opening and displaying a soft ‘knee’ in the opening characteristic (other characteristics may be observed due to contact contamination [3]). A certain shape at this point is desirable since a gentler slope may indicate a tendency of the device to stick during the final application. By applying the indicated allowed contact envelope, a test can be created that actually confirms a required profile on 100% of tested devices. If this check is applied on the waveform already captured once (which is already being used for our timing and contact resistance measurements), there is only a very small time overhead for this ‘envelope’ test (due only to processing time) so effectively this test comes ‘free’.

F. Scales smoothly to life-testing requirements.

Possibly the most interesting of the benefits obtained from this capture method is that it is ideal for monitoring contact switching during life testing. Since life-test switching is only the repeated operate / release cycling of one or more devices with contacts connected to appropriate loads, the contact waveforms are close to those already seen.

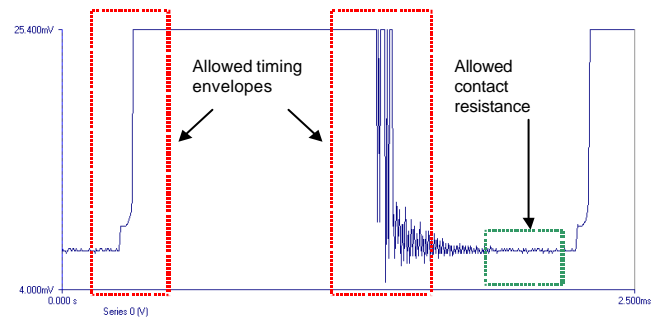


Figure 7. A reed switch contact undergoing life-test at 500Hz, 6V/100mA

Consider Fig. 7 which shows the voltage drop across a reed switch contact undergoing a life-test at 100mA / 6V. With present-day computational power, this captured waveform can be software processed to classify the device as a pass or fail by the application of the timing and contact resistance limit envelopes shown, despite the fact that all of this testing is happening at a cycle rate of 500Hz. Such high-speed testing is

particularly relevant for testing physically small devices and especially at lower load levels.

With the emergence of various micro-machined relay technologies there is an accelerating trend now towards smaller, faster devices with very limited power contacts [4]. This technique is ideal for assessing the contact performance of such parts

G. Obtaining the required waveforms from real contact switching.

So far we have looked at the benefits of digitally processing captured contact waveform data with the assumption that the data is simply the contact voltage drop. Sometimes, for simple measurements it may be possible to utilise only contact voltage drop information but real world situations usually require more work to derive the wanted parameters. For example to adequately cover a range of contact loads from low-levels such as 20mV/10mA up to high power and automotive, a more flexible architecture similar to that of Fig 8 is required.

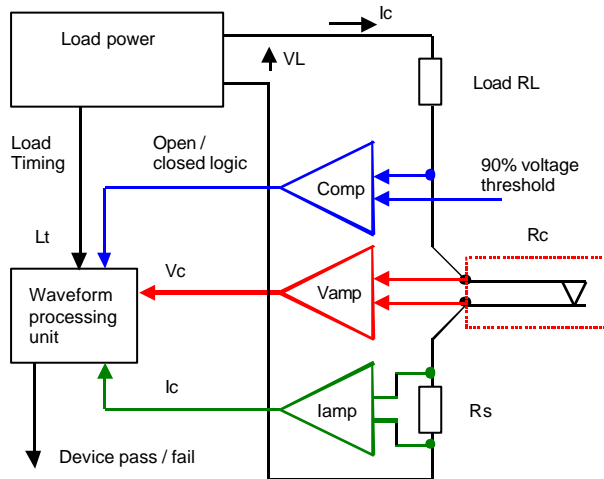


Figure 8. A wide range capture architecture for a contact.

This shows a basic contact environment complete with load power, a load resistor R_L , and a current sensing resistor R_s . In this simple (DC) mode, closure of the contact causes a current $I_c = V_L / R_L$ to flow and the load is chosen to suit the test requirements. While the contact is switching, four separate 'parameters' are digitised and stored as time-variant series:

1. V_c – The contact voltage drop. This is amplified by the preamplifier 'Vamp'.
2. I_c – The contact current. This is amplified by the preamplifier 'Iamp'.
3. OC – The contact open / closed state. This digital logic state is derived by comparing the open-circuit contact voltage with a specified reference level.
4. L_t – An optional load timing signal for AC or other time-variant load supplies.

In a typical load circuit the load resistor R_L cannot always be relied upon for a known value, either because it is of poor initial accuracy, may be subject to self-heating or because it is mounted remotely and lead resistance errors will occur. If we use a current sensing resistor to capture and digitise the contact current we can now derive an accurate contact resistance waveform series where every point is simply:

$$RC \text{ (series)} = VC \text{ (series)} / IC \text{ (series)}$$

Each series here is a collection of points - perhaps 1000 - that covers the actual contact switching period of interest. A typical capture is shown in Fig 9 below. In this figure, the contact voltage drop and the contact current have both been digitised simultaneously, whilst the third trace shows a derived series for contact resistance calculated as above (Note that subsequent processing software must be aware that there are regions of invalid data in the derived contact resistance which must be ignored, for example where the contact current is close to zero).

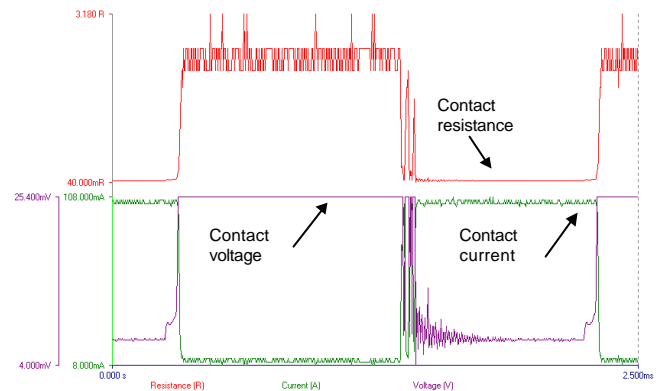


Figure 9. A typical contact switching showing captured contact voltage drop, contact current and derived contact resistance.

In addition to the contact voltage and current waveforms, an additional series – the contact open / closed state – is derived by comparing the open-circuit contact voltage with a specified reference level. Although it would seem possible to utilise the captured contact voltage drop information to imply the contact open / closed state, many specifications call for (say) a 90% threshold on the load voltage for this. Typically, the contact voltage drop preamplifier 'Vamp' must provide gain to ensure that the required contact resistance range and resolution is met – typical gains might be of the order of 100 times - but once this gain is greater than unity the amplifier will saturate and cannot provide information about the contact when the voltage is close to that of the load. However, since we only require to know whether the contact is open or closed as classified against our chosen threshold, we can separately monitor the digital logic open / closed state from the comparator 'Comp'.

Many contact environments require an AC voltage or may have a load voltage which changes during measurement in

some way. When testing low-level contacts, an applied AC load voltage (often 20mV) is used to remove thermoelectric and circuit offset errors from the calculated contact resistance. Other higher power AC loads are simply off-line voltages of 50Hz or 60Hz that will produce corresponding AC contact voltage drops. The result of capturing such voltage and current waveforms produces bipolar data that must be processed in software to remove its AC nature before further calculation of derived resistances can be made.

This processing is quite straightforward in software and can be done using the procedure of ‘Phase-sensitive integration’ as shown in Fig 10. Here we see 2 periods of an original (sine) waveform typically representing the captured contact voltage drop during a stable contact resistance (although it applies equally to captured current waveforms too). The objective is to determine its RMS value, i.e. as if it were a simple DC level. Traditional circuit techniques are slow to determine RMS values because they involve averaging filters that smooth the waveform ripple over many cycles to achieve a stable result. Since this captured waveform is available to us in the form of (say) 1000 sample points, we can use a software algorithm and knowledge of the phase of the waveform (from the ‘load timing’ signal of Fig 8) to construct the rectified waveform ‘2’ by alternate inversion. Finally, waveform ‘3’ is the result of summing all data points of waveform ‘2’ with the final end value being a simple multiple of the original waveform area and hence of its RMS value.

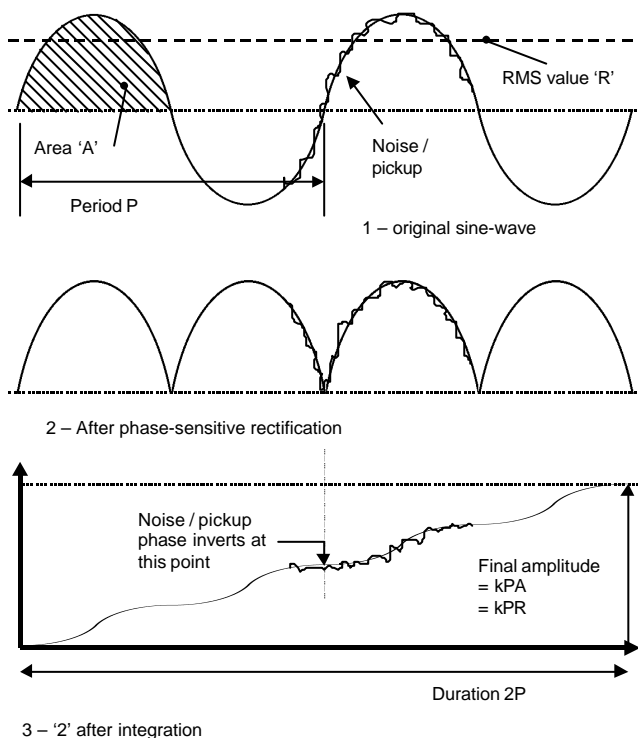


Figure 10. Fast measurement of an AC waveform using phase-sensitive integration.

There are major benefits in using this technique. First, the ‘result’ is available immediately at the end of the test duration (2P above), and second, any noise or pickup is not only

averaged out over the measurement period, but is ‘rejected’ due to the fact that any waveform not in phase with the original will be alternated by the rectification process and after averaging only contributes little to the final ‘DC’ value. Such a technique is also ideal for permitting the user to choose in software the tradeoff between test duration and measurement resolution.

III. PROCESSING GRAPHICAL DATA.

In the previous sections we have seen how it is possible to obtain extensive information from one or more parameters in the form of graphical data, but the task now facing us is to process and present this data to the user in a useful way. Starting with captured graphical data, the user typically requires presentation in two ways:

1. As a ‘single’ parametric result determined algorithmically from the captured data (for example to be compared against pre-set limits) – e.g. ‘Operate time’.
2. As the original captured data displayed for direct viewing (for example as a investigative tool).

The single parametric result in ‘1’ is equivalent to the original single analogue measurement made using classic non-graphical techniques, and will always be required for unattended or production applications. The graphical display of ‘2’ is useful for laboratory investigations or to provide an insight into actual device activity. There is a huge gulf separating these two data presentations, first because the algorithm to determine the parameter is not necessarily implicit from the graphical display, and second because working directly with a block of graphical samples is very much more computationally intensive than handling a single parameter.

For some time we have been employing data capture in our test equipment, mainly for our own benefit in allowing us to derive suitable algorithms that obtain (for example) a single contact resistance value from a specific sample capture of perhaps 1024 samples taken over 20ms. By varying the number of samples and the capture duration, the quality of the single result can be traded against the time taken to complete the measurement but this requires us to ‘embed’ a suitable algorithm that takes the sample series as its input and provides a contact resistance result parameter as its output. Such embedded algorithms are fine where their action is well defined and where any user configuration is planned carefully from the outset, but they are not suitable where significant user flexibility is needed or where information might be required which cannot clearly be foreseen.

An example of this is the plot shown in fig 11 which shows data captured simultaneously for contact open / closed states (top traces) and an applied coil voltage ramp and resulting coil current (bottom traces). Such a display may be of interest to determine certain magnetic circuit characteristics such as contact over-travel. Typically the user will wish to conclude

with a single measured result, perhaps to obtain the difference between the closure of the last normally-open contact and the minimum coil current (relating to the armature closing), however even this difference might be required as a time value, a voltage value or a current value. When one considers that the user may have requirements to measure the difference relative to very specific contact activity such as from 'first closure' or 'last bounce' it is clear that some kind of custom facility is required to permit the user to specify his own measurement 'algorithm'.

With the advent of more powerful processing elements it has now been possible to create a tool that provides flexibility without employing the complex low-level programming techniques that were previously required to process graphical data. The tool is a script-based technique that is both very visual and yet can be automated within production testing. An example of how this script works is shown in the following set of diagrams. Here, a multiple graphics capture shows a smoothly rising coil drive voltage resulting in a collection of contact open / closed traces and a captured coil current waveform. The objective of the example is to measure the coil voltage difference between the last normally-open contact closing and the armature finally coming to rest against the coil assembly (as implied by the lowest point of the dip in the coil current waveform).

In the laboratory, this measurement would be made by 'zooming in' to the area of interest and then manually setting a pair of measurement cursors to quantify the difference. The concept of the script is equally simple since the script actually 'replays' a manually recorded set of cursor positioning functions. This set of example graphs show the various stages of the script.

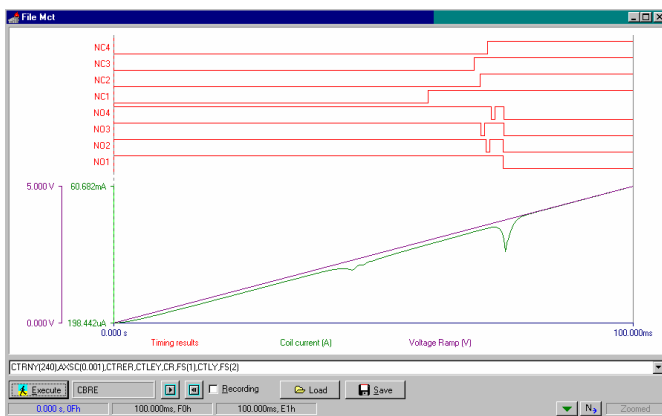


Figure 11. An example of a multiple capture showing contact activity, coil drive voltage ramp and observed coil current.

Fig 11 shows the original captured data before any subsequent processing. It was taken from a 4-pole changeover relay and shows eight contact activity traces together with a rising coil drive voltage ramp and the observed coil current containing a dip at the point where the armature closed.

The first script instruction positions a cursor at the closure of the last normally open contact as shown in Fig 12. This is simply done by specifying the expected contact pattern and the cursor moves to the first occurrence of this pattern. (Various similar functions are provided to allow cursor positioning at the start or end of a group of bounce events as well).

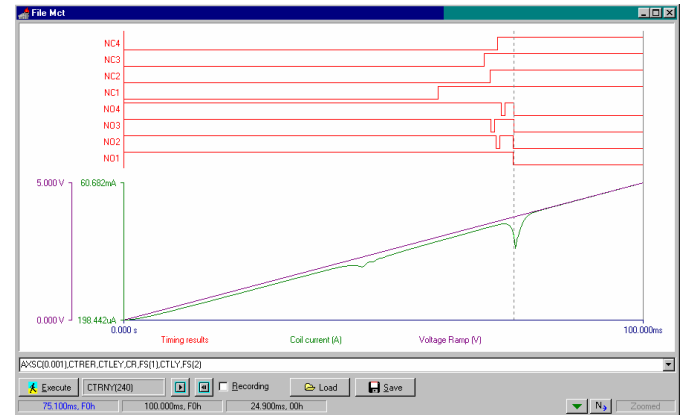


Figure 12. A cursor has been positioned at the closure of the last NO contact.

The next action is to expand the X-axis which more clearly shows the coil current dip and its relationship to the contact activity.

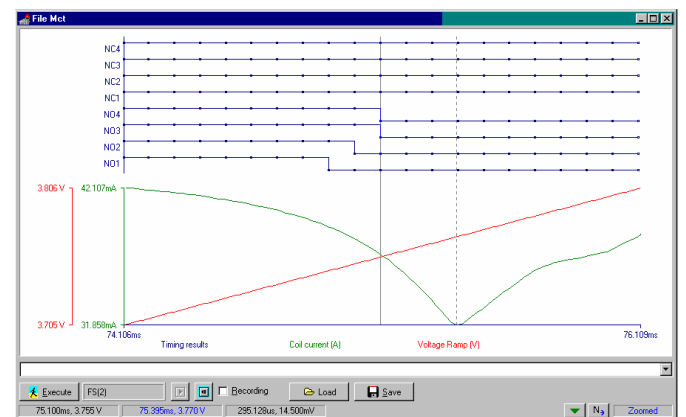


Figure 13. Expanded X-axis around area of interest.

As the script continues to execute, the second (right hand) cursor is positioned at the lowest point on the coil current curve, resulting in the display of Figure 13. At this point, we now have the two cursors located where desired and the final coil voltage difference can be obtained directly from the cursor information. At this point the script is complete and its 'result' is the cursor difference (taken from the active red voltage trace) which is exported back into a simple go/no-go test

where it is compared with programmed limits to pass or fail the device.

To summarise then, the script is automating the same cursor and graphical actions that a user would perform manually, with the difference that the complete script can be executed extremely fast, simply by turning off any screen display of the resulting graphical activity. In this way, the actions illustrated above can be performed in only a few milliseconds, yet if required, the graphical updating can be enabled and the progress of the script to be observed and debugged.

A further example of the flexibility of this tool is shown in the plots of Fig 14 which show three traces of the coil back-emf resulting from the removal of coil current typically to confirm the operation of coil suppression components, showing traces for:

1. No suppression
2. Single diode in parallel across the coil (single diode).
3. Diode in parallel and diode in series (double diode).

The task is to reliably measure the back-emf voltage.

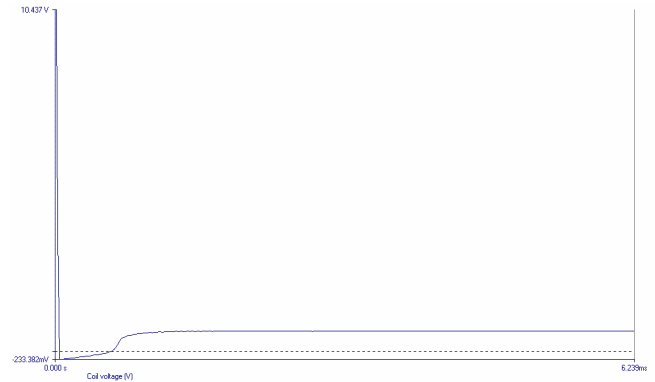
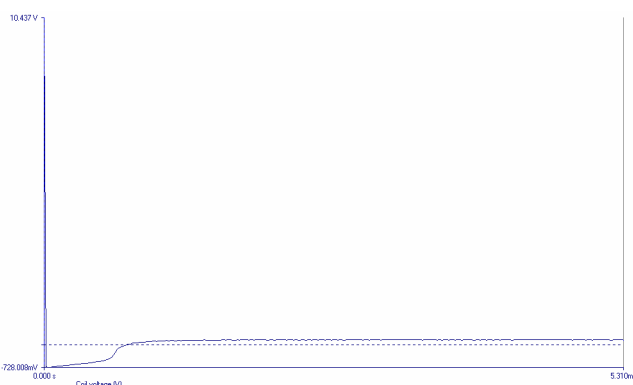
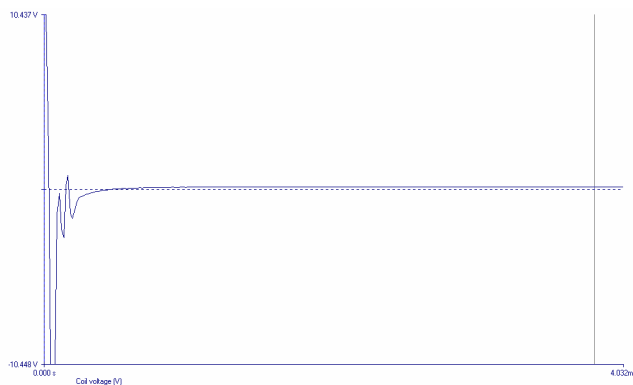


Figure 14a-14c. Coil transient voltages with no diode (top trace) single diode (middle trace) and double diode (bottom trace).

Historically this is a difficult test to implement using hardware alone, because the peak detection hardware that is required can often respond erroneously to other transients as well as that required. Should this happen, debugging the test environment is very difficult because such transients are often intermittent and there is no legacy afterwards other than an incorrect voltage. In Fig 14a-14c however, the coil transient (and any interference) can be clearly seen and easily allows the positioning of a measurement cursor at a chosen time point such as to only measure the wanted coil transient. The double diode case (bottom trace) is the most difficult, where the wanted transient from the parallel diode is masked by the series diode, yet even here it is possible to see and measure the transient cleanly.

CONCLUSION

The technique of employing digitally captured current and voltage waveforms from a switching contact has been shown to provide significant parametric information and together with today's processing power makes it possible to perform real-time analysis of contact effects during switching. The principles outlined have been integrated into a new generation of relay test equipment to further advance the measurement of existing devices and to be ready for the throughput demands of the emerging micro-machined technologies.

ACKNOWLEDGEMENT.

Applied Relay Testing Ltd thanks the following companies for their support: Teledyne Relays (CA, USA), Axicom AG (Switzerland), Siemens EC (Berlin, Germany), Pickering Electronics (UK).

REFERENCES.

- [1] Specification CECC 16000 Figure 7, MIL-R-28776C section 4.8.7.6 etc. (Figure 4), MIL-R-39016E section 4.8.8.4 etc. (figure 4).

- [2] B.J.Frost “A new generation of test equipment” *Proc. of the 45th relay conference, NARM, April 1997*
- [3] Christian N.Neufeld and Werner F.Rieder “Electrical Characteristics of Various Contact Contamination’s.” *IEEE Trans. Comp., Packaging., Manufact. Technol., Vol 18, No 2, June 1995*
- [4] Helmut F.Schlaak et al, “Silicon Microrelay – A Small Signal Relay With Electrostatic Actuator” *Proc. of the 45th relay conference, NARM, April 1997.*